Supplemental Data

Ibrutinib-based therapy reinvigorates CD8$^+$ T cells compared to chemoimmunotherapy: immune-monitoring from the E1912 trial

Despoina Papazoglou et al.

Supplemental Methods

Patient samples and clinical study design. In this study we performed comparative bioassays with samples from the ECOG-ACRIN, NCI-approved E1912 randomized phase 3 clinical trial (ClinicalTrials.gov number NCT02048813). Briefly, the clinical trial included individuals with CLL or the small lymphocytic lymphoma (SLL) presentation of CLL that were 70 years of age or younger with previously untreated but progressive disease according to IWCLL 2008 criteria. Patients with chromosome 17p13 deletion were not eligible given their known poor response to FCR therapy.[1] After providing written informed consent, eligible patients were randomly assigned in a 2:1 ratio to receive ibrutinib daily until disease progression including combination with rituximab up to cycle 7 (ibrutinib-rituximab) or traditional fludarabine, cyclophosphamide and rituximab (FCR) chemoimmunotherapy for 6 cycles (**supplemental Figure 1**).[2] Eighty-nine (89) patients treated with ibrutinib-rituximab and sixty-two (62) patients treated with FCR participating in the trial, were randomly selected for immune monitoring, functional and correlative analysis studies for this present study report. Peripheral Blood Mononuclear Cells (PBMCs) from patients treated with either ibrutinib-rituximab or FCR were biobanked longitudinally at three time-points: prior to treatment (baseline, "B/L"), 6 months ("6M") and 12 months ("12M") on-therapy to allow batched laboratory studies. Additionally, baseline (B/L)

and 18 months ("18M") later time-point (n=5 for each arm) samples were used to assess differences in T cell cytotoxic function.

E1912 trial clinical outcome monitoring. Progression Free Survival (PFS), defined as the time from randomization to documented progression or death without documented progression, incidence of any infection (grade of infections occurring in the trial are summarized in **supplemental Table 4**) and minimal residual disease (MRD) were assessed as part of this study.[2,3] Median follow-up for PFS was 43.6 months from randomization. Overall, among the 88 patients in the ibrutinib-rituximab arm and 54 patients in the FCR arm studied as part of the immune subset and PFS correlation analysis, 13 patients on each arm experienced disease progression/PFS event. The incidence of infection was monitored during patient follow-up according to the protocol. MRD was measured by 8-color flow cytometry analysis of peripheral blood as previously described[4] at the following time-points from treatment initiation: ibrutinib-rituximab arm: 12, 24 and 36 months and FCR: 3, 12, 24 and 36 months.

Patient cell isolation and cell culture. Highly viable PBMCs were isolated via density gradient centrifugation with Ficoll-Paque Plus (GE Healthcare), washed twice with RPMI (1640 1x, Gibco by Thermo Fisher Scientific) and viably frozen in 90% fetal bovine serum (FBS) (Life Technologies) supplemented with 10% dimethyl sulfoxide (DMSO) (Sigma-Aldrich) for storage in liquid nitrogen. For functional bioassays, patient $CD3^+$, $CD4^+$ and $CD8^+$ T cells from baseline and treatment time-points were negatively isolated using column-free, magnetic separation following initial positive selection depletion of $CD19^+$ CLL B cells (Thermo Fisher Scientific kits). In parallel, $CD19^+$ CLL B cells were negatively isolated from B/L patient samples to act as target autologous tumor cells. Lymphocyte purity and viability following their enrichment were determined by flow cytometry for both treatment arms using a >90% and >80% cut-off

respectively for all downstream functional analysis. Primary immune cells were cultured in AIM-V (Thermo Fisher Scientific) medium for up to two days.

Antibodies and reagents (flow cytometry and T cell assays). directly conjugated antibodies (Abs) were obtained from BD Bioscience unless stated otherwise: CCR7 (CD197)-V450 Clone-150503, CD3-V500 Clone-UCHT1, CD45-RA-AF488 Clone-L48, CD4-PE-Cy7 Clone-SK3, PD-1 (CD279)-APC Clone-MIH4, CD8-APC-H7 Clone-SK1, CD19-V450 Clone-HIB19, PD-L1 (CD274)-FITC Clone-MIH1, PD-L1-V510 Clone-MIH1, CD56-PE-Cy7 Clone-B159, CD16-APC-H7 Clone 3G8, CD25-V450 Clone-MA251, CXCR3 (CD183)-FITC Clone-1C6, CCR6 (CD196)-PE Clone-11A9, CD-127-PERCP-Cy5.5 Clone-A019D5 (BioLegend), HLA-DR-APC-H7 Clone-L243.

IF for T cell:CLL cell conjugate assays utilized: cell tracker Blue CMAC (7-amino-4 chloromethylcoumarin), rhodamine phalloidin, Alexa Fluor 647-labeled goat anti-rabbit and Alexa Fluor 488-labeled goat anti-mouse secondary antibodies (Thermo Fisher Scientific). Rabbit anti-human Granzyme B (GrB) (ab53097) (Abcam), mouse anti-human phosphotyrosine (pTyr) (4G10) (05-321) (Millipore), Alexa Fluor 700-labeled mouse anti-human CD8 (SK1) (Biolegend) and goat anti-human CD4 (polyclonal) (Novus Bio). T cell-mediated cytotoxicity assay: staphylococcal superantigens' cocktail (sAgs) (SEA and SEB, Sigma-Aldrich). Functional grade Abs anti-CD3 (OKT3) and anti-CD28 (CD28.2), TO-PRO-3 Iodide 1mM solution in DMSO (viability dye), CellTrace™ CFSE (Thermo Fisher Scientific). Anti-PD-1 (Ultra-LEAF™) and anti-PD-L1 (Ultra-LEAF™) and isotype controls (BioLegend). T cell-engaging bispecific antibodies CD20xCD3 (CD20-TCB, glofitamab) and DP47-TCB antibody control (Roche Glycart AG).[5]

Flow cytometric analysis. Results are expressed as absolute number of cells expressing antigens of interest calculated from the percentage of positive cells and the absolute lymphocyte count (ALC) of the blood sample at the time of collection (or percentage of positive cells expressing the antigen of interest). For every subset analyzed with flow cytometry, we calculated the

numbers based on the following formula: Absolute (Abs) subset= Lymphocyte Cell count x percent subset. Results were corrected for any background staining using isotype controls during compensation setup for all multi-color panels (supplemental Table 3). Frozen PBMCs were thawed, washed twice with phosphate-buffered saline (PBS), and resuspended in 500-1000 µL PBS containing 1% bovine serum albumin (BSA) at a concentration of 1-2 × 10^6. Dead cells were removed using a Dead-cell removal kit following the manufacturer's instructions (Miltenyi Biotec Inc.) prior to incubation with the fluorochrome-conjugated antibodies at room temperature in the dark for 20 min. After washing, cells were fixed in 500 µL of BD Stabilizing Fixative. Stained samples were run the same day on a BD FACSCanto II flow cytometer (BD Biosciences). T cell subset result analysis was performed using Kaluza software Version 1.5a (Beckman Coulter). $CD4^+$ and $CD8^+$ T cells were categorized into naïve ($T_{naïve}$), central memory (T_{CM}), effector memory (T_{EM}) and terminally differentiated effector memory (T_{EMRA}) T subsets based on the membranous expression of CD45RA and CCR7. Subsequently, PD-1 and PD-L1 protein expression was measured for all $CD4^+$ and $CD8^+$ subsets. Helper $CD4^+$ T cells were further characterized into T_H1, T_H2, T_H17, T_{Regs} and activated T_{Regs} based on the expression of CXCR3, CCR6, CD127, CD25 and HLA-DR. The gating strategies used are presented in supplemental Table 3. Quantitative flow cytometry-based T cell-mediated cytotoxicity results were analyzed using FlowJo Version 10.4.1 (TreeStar).

T cell-mediated anti-CLL cytotoxicity assay. Negatively selected $CD3^+$ T cells from baseline and both on-therapy time-points (6M, 12M from each clinical treatment arm) were plated with 1 µg/mL anti-human CD28 antibody in 48-well plates previously coated with 1 µg/mL anti-human CD3 antibody for 48 hours at 37°C to allow effector T cell activation prior to cytotoxicity assays. To investigate immune checkpoint blockade antibodies, $CD3^+$ T cells were also co-treated with anti-PD-L1 or anti-PD-1 antibodies (10 µg/mL) or isotype controls (together with anti-CD3 + anti-CD28) for 48 hours. On the day of the assay, autologous baseline (B/L) negatively selected

$CD19^+$ CLL B cells were stained with CellTrace™ CFSE (200 nM) to act as identical targets (and allow accurate evaluation of changes in T-cell function with therapy) (for immune checkpoint blockade, these CFSE-stained baseline $CD19^+$ CLL B cells were also pre-treated with anti-PD-L1 or anti-PD-1 (10 μg/mL) or isotype controls for 1 hour prior to cytotoxicity assays). Target CLL B cells (tumor cells) were then pulsed with 2 μg/mL superantigen (sAg) (SEA and SEB, Sigma-Aldrich) for 30 min at 37°C. Next, these target CLL B cells (2.5×10^4) were added to the pre-activated effector T cells at a 1:20 (Target: Effector) ratio, centrifuged and incubated for 4 hours at 37°C. Target cells alone were incubated as a control for spontaneous cell death. Cells were stained with TO-PRO-3 viability dye (Thermo Fisher Scientific) according to the manufacturer's instructions and T cell-mediated specific CLL B cell death was determined by flow cytometry on BD FACSCanto II flow cytometer (BD Biosciences). Cytotoxicity was calculated as follows: % of T cell-mediated tumor cell death = (% $CFSE^+$ TO-PRO-3^+ target cells incubated with effector T cells - % of $CFSE^+$ TO-PRO-3^+ target cells incubated alone) × 100 / (100 - % of $CFSE^+$ TO-PRO-3^+ target cells incubated alone).

To test the efficacy of the CD20xCD3 bispecific antibody (CD20-TCB/ RG6026/ glofitamab, Roche Glycart AG), negatively selected $CD3^+$ T cells from all time-points were cultured with CFSE-stained negatively selected baseline $CD19^+$ CLL B cells in the presence of CD20xCD3 (0.01 μg/mL) or a non-specific binding control antibody (DP47-TCB, 0.01 μg/mL). T cell-mediated anti-CLL cytotoxicity induced by glofitamab was calculated after 24 hours via flow cytometry as described above.

T cell:CLL (tumor B) cell conjugation and immunological synapse assays. Cell conjugate assays were performed as previously described.[6,7] Negatively selected untreated (baseline) $CD19^+$ CLL B cells were stained with CellTrace™ Blue CMAC (Invitrogen) according to the manufacturer's instructions. CMAC stained $CD19^+$ cells (1×10^6) were then pooled with equal number of autologous negatively selected $CD3^+$ T cells from untreated (B/L), ibrutinib-rituximab or FCR

treated PBMCs samples (6M, 12M), centrifuged at 260g (5 min) and incubated at 37°C for 15 min. Cells were transferred onto microscope slides (Polysine slides; Thermo Fisher Scientific) using a cell concentrator (Cytofuge 2) and fixed for 15 min at room temperature with 3% methanol-free formaldehyde (Thermo Fisher Scientific) in PBS.

IF staining and confocal microscopy. IF labeling was done using Cytofuge2 cell concentrator units as previously described.[8] Following fixing, cells were permeabilized with 0.3% Triton X-100 (Sigma-Aldrich) in PBS for 5 min and treated for 10 min with 5% goat serum (Sigma-Aldrich) in PBS blocking solution. Primary and secondary Abs (Alexa Fluor 488 or 647, Thermo Fisher Scientific) were applied sequentially for 1 hour and 30 min respectively at 4°C in 5% goat serum in PBS blocking solution. F-actin was stained with rhodamine phalloidin (Thermo Fisher Scientific) following the manufacturer's instructions and applied with the secondary Abs. After washing the cell specimens were sealed with coverslips using fluorescent mounting medium FluorSaveTM reagent (Merk Millipore). Apropriate dilutions of isotype-control, primary Abs and subsequent fluorescent secondary Abs were used to optimize the specificity of the staining. Medial optical section (or Z-stacks for 3D volume images) images were captured with a high-sensitivity A1R confocal microscope using a 63X/1.40 oil objective with the NIS- Elements software Version 5.01 (Nikon). Image sets to be compared (B/L, 6M, 12M) were acquired during the same session using identical acquisition settings. Fluorescence was acquired sequentially to prevent passage of fluorescence from other channels (DU4 sequential acquisition). Detectors were set to detect an optimal signal below saturation limits.

Quantitative image analysis at T cell synapses. Blinded confocal images (n=3 per time-point per patient sample) were analyzed using the NIS-Elements image analysis software Version 5.01 (Nikon). T cell:CLL cell conjugates were identified only when T cells were in direct contact interaction with CLL B cells (CMAC stained, blue fluorescent channel). To measure the polarized

recruitment of F-actin (red fluorescent channel) and granzyme B (GrB) at T:CLL cell immune synapses (or contact sites), regions of interest (ROI) were drawn around i) the conjugation contact site of T cell:CLL cells, ii) the regions of the T cell not in contact with CLL B cells and iii) a background non-cell image area. The relative recruitment index (RRI) was calculated as: (MFI at the contact site or immune synapse - background) / (MFI at the T cell membrane not in contact with the CLL B cell - background). When T cells formed F-actin polarized immune synapses with CLL cells, the RRI value was greater than 1, whereas non-polarized F-actin immune synapses showed an RRI value of below or equal to 1. The median F-actin RRI value per patient sample (time-point) from the total analyzed T cell:CLL conjugates was used to provide a cut-off point to define "strong" versus "weak" immune synapses with: RRI > the median defined as "strong", whereas when the RRI < median, the immune synapse was defined as "weak". The accumulation of phosphotyrosine (pTyr) to T:CLL cell immune synapses was calculated using Sum Intensity analysis at T cell:CLL immune synapse/contact site ROIs (NIS-elements imaging software). To investigate the $CD8^+$ T cell lytic versus $CD4^+$:CLL synapses, the number of immune conjugates formed between $CD8^+$ and $CD4^+$ T cells and CLL cells was calculated out of the total number of all synapses per image (field of view) using manual counting. All T cell contact sites and immune synapses with CLL B cells per confocal image (maximum n=30 conjugates/synapses per image) were analyzed. To generate final data plots, the mean RRI value of T cell:CLL conjugates from all three images analyzed per patient treatment time-point was calculated. Data were then exported into Prism Version 9 software (GraphPad) for statistical analysis.

Statistical analysis and correlation studies. Statistical analysis for the functional T cell cytotoxicity and immune synapse assays was performed using GraphPad Prism version 9 software. Immune monitoring flow cytometry analysis results were analyzed using R version 3.5.2. For the flow cytometry results, statistical differences between baseline (B/L) and on-

treatment (6M, 12M) time-points and between the 6M and 12M time-points were calculated using the Wilcoxon signed-rank test. Multiple comparisons ANOVA test was used to assess differences (6M, 12M time-points vs. B/L) in the percentage of $CD4^+$/ $CD8^+$: CLL immune conjugates. Cox proportional hazards models were used to assess correlations between the immune cell subset data and PFS (flow cytometry analysis, median marker values were used as cut-off point for each time-point). One hundred and twenty-two (122) immune cell subsets were analysed for their correlation with PFS. Only immune cell subsets found to have statistically significant association are presented in Figure 1. In addition, multivariable analysis was then performed using Cox models with PFS as the outcome variable and the statistically significant subsets and CLL IPI risk category included as covariates in the ibrutinib-rituximab arm (CLL-IPI data was available for n=83 patients (low IPI n=8, intermediate IPI n=25, high IPI n=41, very high IPI n=9)) (Supplemental Table 4). The association between F-actin RRI at $CD4^+$ T cell immune synapse interactions with CLL cells and PFS was assessed using Cox proportional hazards models, with median values of F-actin RRI (total analyzed T cell:CLL conjugates) used as the cut-off point (> the median - the immune synapse was defined as "strong", < the median - defined as "weak").

Wilcoxon test was used to identify significant associations of immune cell subset data (flow cytometry analysis, continuous data) and patients' infection status (any infection vs no infection). Anti-CLL T cell killing function (cytotoxicity) and T cell immune synapse function data were compared between patients with different grades of infection to those not experiencing infections using Wilcoxon tests. Supplemental Table 5 presents the distribution of infections (grades) for the entire E1912 trial, while supplemental Tables 6 and 7 summarize the distribution of infections (grades) that occurred in the patients whose samples were used for the T cell-mediated anti-CLL cytotoxicity assays and immune synapse formation functional assays and correlation analysis. MRD and immune cell subset data (flow cytometry analysis) associations were assessed using Spearman correlation (ranked individual data points analysis).

P values ≤.05 were considered significant.

Data sharing

For original data and protocols, please contact the corresponding author.

Supplemental Data References

1. Stilgenbauer S, Schnaiter A, Paschka P, et al. Gene mutations and treatment outcome in chronic lymphocytic leukemia: results from the CLL8 trial. Blood. 2014;123(21):3247-3254.

2. Shanafelt TD, Wang XV, Kay NE, et al. Ibrutinib-Rituximab or Chemoimmunotherapy for Chronic Lymphocytic Leukemia. N Engl J Med. 2019;381(5):432-443.

3. Shanafelt TD, Wang XV, Hanson CA, et al. Long-term outcomes for ibrutinib-rituximab and chemoimmunotherapy in CLL: updated results of the E1912 trial. Blood. 2022;140(2):112-120.

4. Wang V, Hanson CA, Tschumper R, et al. Measurable Residual Disease Does Not Preclude Prolonged Progression-free Survival in CLL Treated with Ibrutinib. Blood. 2021.

5. Bacac M, Colombetti S, Herter S, et al. CD20-TCB with Obinutuzumab Pretreatment as Next-Generation Treatment of Hematologic Malignancies. Clin Cancer Res. 2018;24(19):4785-4797.

6. Ramsay AG, Johnson AJ, Lee AM, et al. Chronic lymphocytic leukemia T cells show impaired immunological synapse formation that can be reversed with an immunomodulating drug. J Clin Invest. 2008;118(7):2427-2437.

7. Chiu H, Trisal P, Bjorklund C, et al. Combination lenalidomide-rituximab immunotherapy activates anti-tumour immunity and induces tumour cell death by complementary mechanisms of action in follicular lymphoma. Br J Haematol. 2019;185(2):240-253.

8. Ioannou N, Hagner PR, Stokes M, et al. Triggering interferon signaling in T cells with avadomide sensitizes CLL to anti-PD-L1/PD-1 immunotherapy. Blood. 2021;137(2):216-231.

Supplemental Tables

Supplemental Table 1. Clinical characteristics of the E1912 patients randomly selected for the functional and correlative studies used in this report

Variable	Category	IR	FCR	Total	*P*-value
Total		**89**	**62**	**151**	-
Age	Mean (SD) Median (Q1,Q3) [Min, Max] Freq. of Missing	56.7 (7.7) 58.0 (52.0,61.0) [31.0,70.0] 0	55.8 (7.4) 57.0 (52.2,60.0) [28.0,69.0] 0	56.3 (7.6) 58.0 (52.0,61.0) [28.0,70.0] 0	0.327
Age, category	<60 >=60 Unknown/Missing	54 (60.7) 35 (39.3) 0	43 (69.4) 19 (30.6) 0	97 (64.2) 54 (35.8) 0	0.304
Gender	Female Male Unknown/Missing	26 (29.2) 63 (70.8) 0	18 (29.0) 44 (71.0) 0	44 (29.1) 107 (70.9) 0	1.000
RAI Stage	Low, 0 Intermediate, I-II High, III-IV Unknown/Missing	1 (1.1) 55 (61.8) 33 (37.1) 0	6 (9.7) 37 (59.7) 19 (30.6) 0	7 (4.6) 92 (60.9) 52 (34.4) 0	0.049
ECOG PS	0 1 2 Unknown/Missing	54 (60.7) 33 (37.1) 2 (2.2) 0	33 (53.2) 28 (45.2) 1 (1.6) 0	87 (57.6) 61 (40.4) 3 (2.0) 0	0.604
Hemoglobin, g/dL	Mean (SD) Median (Q1,Q3) [Min, Max] Freq. of Missing	12.1 (2.1) 12.3 (11.0,14.0) [4.4,15.9] 0	12.3 (2.0) 12.6 (11.2,13.6) [7.0,17.6] 2	12.2 (2.1) 12.4 (11.1,13.9) [4.4,17.6] 2	0.662
Platelets, 10^3/µL	Mean (SD) Median (Q1,Q3) [Min, Max] Freq. of Missing	152.2 (68.0) 146.0 (109.0,189.0) [20.0,435.0] 0	166.3 (87.5) 145.0 (106.0,206.2) [38.0,485.0] 0	158.0 (76.7) 146.0 (108.0,190.5) [20.0,485.0] 0	0.555
WBC, 10^3/µL	Mean (SD) Median (Q1,Q3) [Min, Max] Freq. of Missing	120.5 (114.0) 92.7 (27.4,170.5) [3.2,597.7] 0	103.6 (103.3) 57.6 (18.4,187.5) [3.7,434.1] 0	113.6 (109.7) 78.8 (24.4,180.2) [3.2,597.7] 0	0.327
Beta-2 Microglobulin, mg/L	Mean (SD) Median (Q1,Q3) [Min, Max] Freq. of Missing	4.4 (2.0) 4.1 (3.0,5.3) [1.7,12.4] 0	4.0 (1.7) 3.8 (2.7,4.8) [1.8,10.3] 0	4.3 (1.9) 4.0 (2.8,5.2) [1.7,12.4] 0	0.217
Creatinine Clearance (mL/min)	Mean (SD) Median(Q1,Q3) [Min, Max] Freq. of Missing	96.8 (31.5) 88.5 (76.2,111.6) [47.6,220.1] 1	117.0 (50.2) 101.5 (84.3,143.2) [50.8,331.4] 0	105.2 (41.4) 94.5 (76.9,121.8) [47.6,331.4] 1	0.009
Coombs Test	Negative Positive Unknown/Missing	81 (92.0) 7 (8.0) 1	56 (91.8) 5 (8.2) 1	137 (91.9) 12 (8.1) 2	1.000
Splenomegaly	No Yes Unknown/Missing	51 (57.3) 38 (42.7) 0	34 (54.8) 28 (45.2) 0	85 (56.3) 66 (43.7) 0	0.868
Lymphadenopathy	No Yes Unknown/Missıng	28 (31.5) 61 (68.5) 0	22 (35.5) 40 (64.5) 0	50 (33.1) 101 (66.9) 0	0.725
Del (11q22.3)	Abnormal Normal Unknown/Missing	25 (28.4) 63 (71.6) 1	17 (27.4) 45 (72.6) 0	42 (28.0) 108 (72.0) 1	1.000
Dohner classification	del(17p) del(11q22) trisomy 12 normal del(13q) other Unknown/Missing	0 (0.0) 25 (28.1) 14 (15.7) 16 (18.0) 32 (36.0) 2 (2.2) 0	0 (0.0) 17 (27.4) 10 (16.1) 11 (17.7) 22 (35.5) 2 (3.2) 0	0 (0.0) 42 (27.8) 24 (15.9) 27 (17.9) 54 (35.8) 4 (2.6) 0	1.000
IGHV	Mutated Unmutated Unknown/Missing	17 (20.0) 68 (80.0) 4	19 (36.5) 33 (63.5) 10	36 (26.3) 101 (73.7) 14	0.045

Supplemental Table 2. Clinical characteristics of the patients used in the functional/correlative work in comparison to the total patients enrolled in the E1912 trial				
Variable	**Category**	**No sample**	**Sample included**	**P-value**
Total		**378**	**151**	**-**
Age	Mean (SD) Median (Q1,Q3) [Min, Max] Freq. of Missing	56.9 (7.3) 58.0 (52.0,61.0) [29.0,70.0] 0	56.3 (7.6) 58.0 (52.0,61.0) [28.0,70.0] 0	0.366
Age, category	<60 >=60 Unknown/Missing	217 (57.4) 161 (42.6) 0	97 (64.2) 54 (35.8) 0	0.107
Gender	Female Male Unknown/Missing	129 (34.1) 249 (65.9) 0	44 (29.1) 107 (70.9) 0	0.305
RAI Stage	Low, 0 Intermediate, I-II High, III-IV Unknown/Missing	13 (3.4) 189 (50.0) 176 (46.6) 0	7 (4.6) 92 (60.9) 52 (34.4) 0	0.034
ECOG PS	0 1 2 Unknown/Missing	248 (65.6) 121 (32.0) 9 (2.4) 0	87 (57.6) 61 (40.4) 3 (2.0) 0	0.174
Hemoglobin, g/dL	Mean (SD) Median (Q1,Q3) [Min, Max] Freq. of Missing	12.1 (2.2) 12.4 (10.5,13.8) [5.5,17.5] 7	12.2 (2.1) 12.4 (11.1,13.9) [4.4,17.6] 2	0.641
Platelets, 10^3/µL	Mean (SD) Median (Q1,Q3) [Min, Max] Freq. of Missing	158.0 (72.6) 150.0 (105.0,203.8) [9.6,508.0] 0	158.0 (76.7) 146.0 (108.0,190.5) [20.0,485.0] 0	0.718
WBC, 10^3/µL	Mean (SD) Median (Q1,Q3) [Min, Max] Freq. of Missing	107.4 (116.5) 70.4 (20.8,151.1) [1.6,672.0] 0	113.6 (109.7) 78.8 (24.4,180.1) [3.2,597.7] 0	0.226
Beta-2 Microglobulin, mg/L	Mean (SD) Median (Q1,Q3) [Min, Max] Freq. of Missing	3.9 (2.0) 3.4 (2.5,4.5) [1.0,14.4] 5	4.3 (1.9) 4.0 (2.8,5.2) [1.7,12.4] 0	0.002
Creatinine Clearance (mL/min)	Mean (SD) Median(Q1,Q3) [Min, Max] Freq. of Missing	100.1 (31.6) 96.9 (77.3,118.2) [41.0,217.5] 20	105.2 (41.4) 94.5 (76.9,121.8) [47.6,331.4] 1	0.709
Coombs Test	Negative Positive Unknown/Missing	336 (92.8) 26 (7.2) 16	137 (91.9) 12 (8.1) 2	0.714
Splenomegaly	No Yes Unknown/Missing	226 (59.8) 152 (40.2) 0	85 (56.3) 66 (43.7) 0	0.494
Lymphadenopathy	No Yes Unknown/Missıng	109 (28.8) 269 (71.2) 0	50 (33.1) 101 (66.9) 0	0.346
Del (11q22.3)	Abnormal Normal Unknown/Missing	75 (19.9) 302 (80.1) 1	42 (28.0) 108 72.0) 1	0.049
Dohner classification	del(17p) del(11q22) trisomy 12 normal del(13q) other Unknown/Missing	2 (0.5) 75 (19.8) 73 (19.3) 79 (20.9) 125 (33.1) 24 (6.3) 0	0 (0.0) 42 (27.8) 24 (15.9) 27 (17.9) 54 (35.8) 4 (2.6) 0	0.167
IGHV	Mutated Unmutated Unknown/Missing	78 (30.2) 180 (69.8) 120	36 (26.3) 101 (73.7) 14	0.484

Supplemental Table 3. Immunophenotyping (gating strategy) of immune subsets	
Immune cell type	**Markers**
Naïve ($T_{naïve}$)	$CD3^+$, $CD4^{+/-}$, $CD8^{-/+}$, $CD45RA^+CCR7^+$
Central memory (T_{CM})	$CD3^+$, $CD4^{+/-}$, $CD8^{-/+}$, $CD45RA^-CCR7^+$
Effector memory (T_{EM})	$CD3^+$, $CD4^{+/-}$, $CD8^{-/+}$, $CD45RA^-CCR7^-$
Terminally differentiated (T_{EMRA})	$CD3^+$, $CD4^{+/-}$, $CD8^{-/+}$, $CD45RA^+CCR7^-$
T helper 1 (T_H1)	$CD3^+$, $CD4^+$, $CXCR3^+CCR6^-$
T helper 2 T_H2	$CD3^+$, $CD4^+$, $CXCR3^-CCR6^-$
T helper 17 T_H17	$CD3^+$, $CD4^+CXCR3^-CCR6^+$
T regulatory (T_{reg})	$CD3^+$, $CD4^+$, $CD127(dim)^+CD25^+$
Activated T_{Reg}	$CD3^+$, $CD4^+$, $CD127(dim)^+CD25^+HLA\text{-}DR^+$
Natural killer (NK)	$CD3^-$, $CD56^+$ ($CD16^+$)

Supplemental Table 4. Multivariable model: Immune subsets with CLL-IPI score. Hazard Ratio (HR) is for marker high/marker low (median cutoff). CLL-IPI low and intermediate combined into low (n=33). CLL-IPI high and very high combined into high (n=50).

Green rows (correlations with Hazard Ratio (HR) values < 1) indicate higher immune subsets associated with longer PFS, while higher immune subsets associating with shorter PFS (HR > 1) are highlighted in blue rows (from Figure 1D).

B/L				
Immune Subset	HR	Lower.95	Upper.95	*P*-value
PD-1^+ $CD8^+$ T_{EM} ab	0.702	0.151	3.255	0.651
$CD4^+$ T_{EM} ab	0.631	0.124	3.207	0.578
T_{Regs} of $CD4^+$ ab	1.109	0.208	5.911	0.903
PD-1^+ $CD4^+$ ab	0.815	0.173	3.832	0.795
% PD-$L1^+$ $CD19^+$	0.050	0.006	0.410	0.005
% $CD8^+$ T_{naive} of $CD8^+$	4.592	0.815	25.866	0.084
% T_H2 of $CD3^+$	2.388	0.536	10.644	0.254
CLL-IPI (high vs low)	0.861	0.265	2.794	0.803
6M				
Immune Subset	HR	Lower.95	Upper.95	p-value
% T_{EM} of $CD8^+$	0.384	0.103	1.429	0.153
$CD8^+$ T_{CM} ab	3.906	1.050	14.525	0.042
% T_H2 of $CD3^+$	3.045	0.754	12.291	0.118
CLL-IPI (high vs low)	0.841	0.260	2.721	0.773

Higher levels associated with longer PFS
Higher levels associated with shorter PFS
CLL-IPI score does not associate with PFS

Supplemental Table 5. Distribution of infections across all patients enrolled in E1912 trial							
	Total	**Grade of infection**					
		0*	**1**	**2**	**3**	**4**	**5**
IR	354	152	7	157	33	5	0
FCR	175	120	0	39	10	5	1
*0=no infections							

Supplemental Table 6. Distribution of infections across patients whose samples used in the T cell-mediated cytotoxicity assays							
	Total	**Grade of infection**					
		0*	**1**	**2**	**3**	**4**	**5**
IR	39	18	0	18	3	0	0
FCR	26	15	0	8	1	2	0
*0=no infections							

Supplemental Table 7. Distribution of infections across patients whose samples used in T cell immune synapse formation assays							
	Total	**Grade of infection**					
		0*	**1**	**2**	**3**	**4**	**5**
IR	52	25	0	23	4	0	0
FCR	45	25	0	12	5	3	0
*0=no infections							

Supplemental Figures

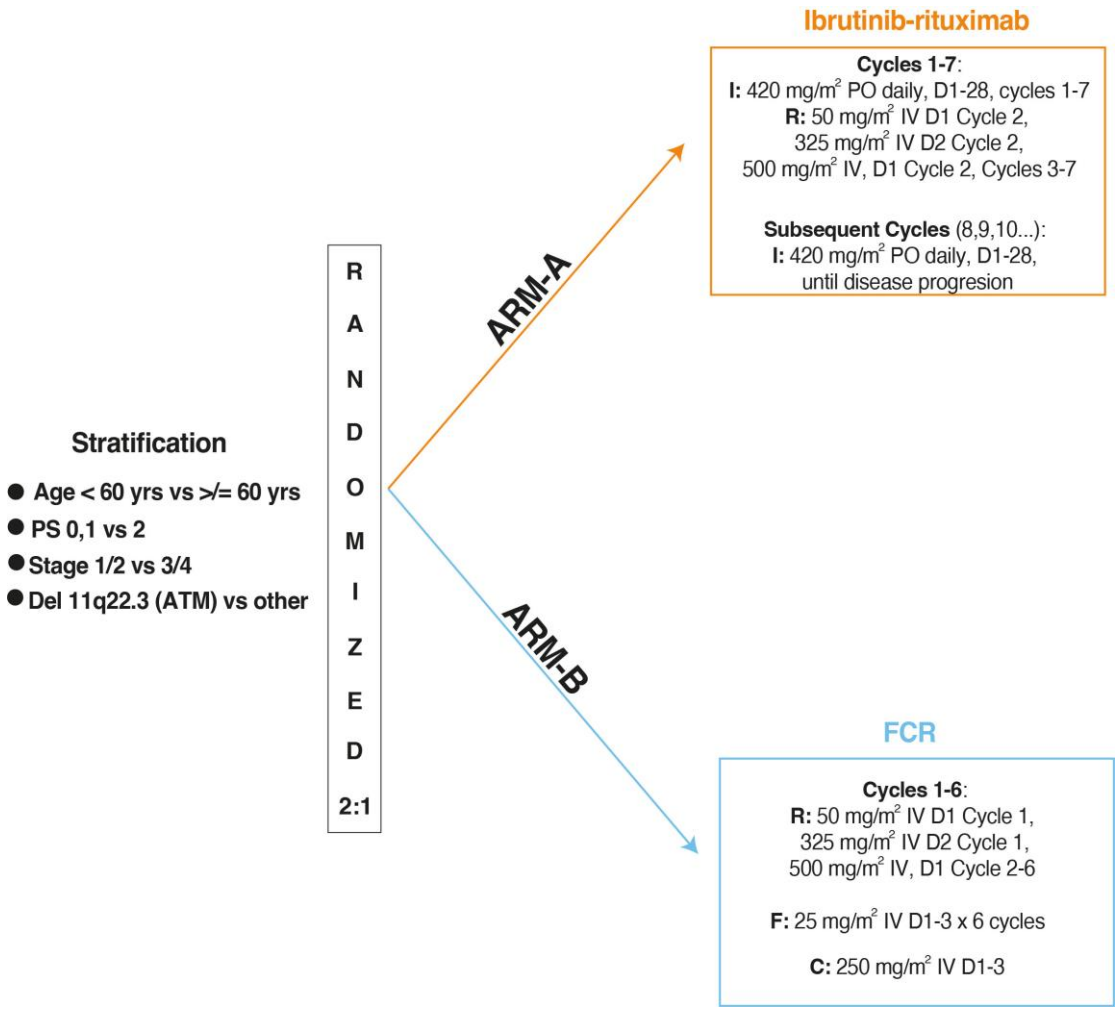

Supplemental Figure 1. Schematic of the E1912 phase 3 randomized clinical trial design. Each cycle is 28 days. Yrs, years; PS, Performance Status (ECOG); ATM, ataxia-telangiectasia mutated gene; PO, Per os (oral administration); D, Day; I, Ibrutinib; R, Rituximab; F, Fludarabine; C, Cyclophosphamide.

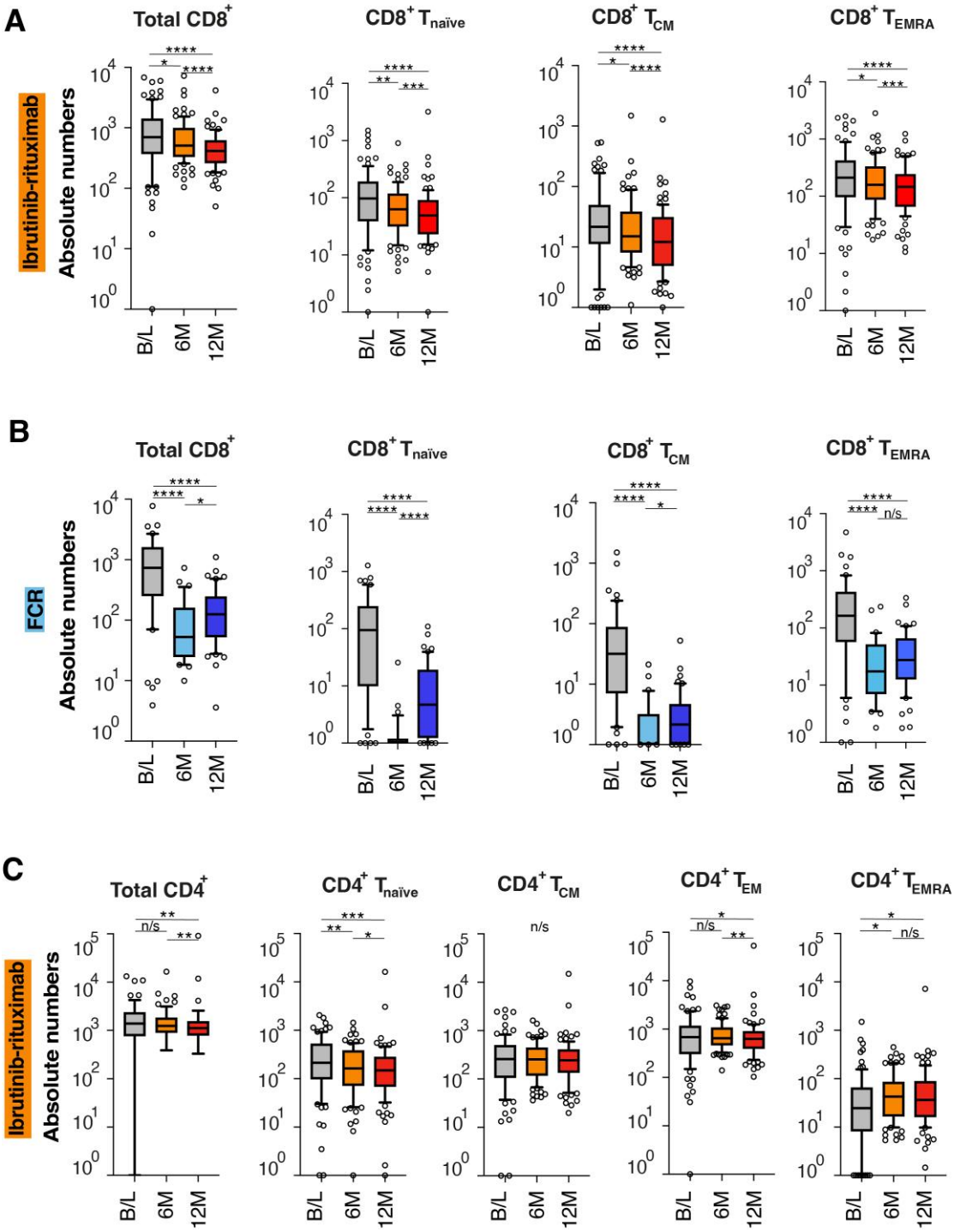
A
Total CD8+
CD8+ Tnaïve
CD8+ TCM
CD8+ TEMRA
Ibrutinib-rituximab
Absolute numbers
B/L
6M
12M
B
Total CD8+
CD8+ Tnaïve
CD8+ TCM
CD8+ TEMRA
FCR
Absolute numbers
C
Total CD4+
CD4+ Tnaïve
CD4+ TCM
CD4+ TEM
CD4+ TEMRA
Ibrutinib-rituximab
Absolute numbers
n/s

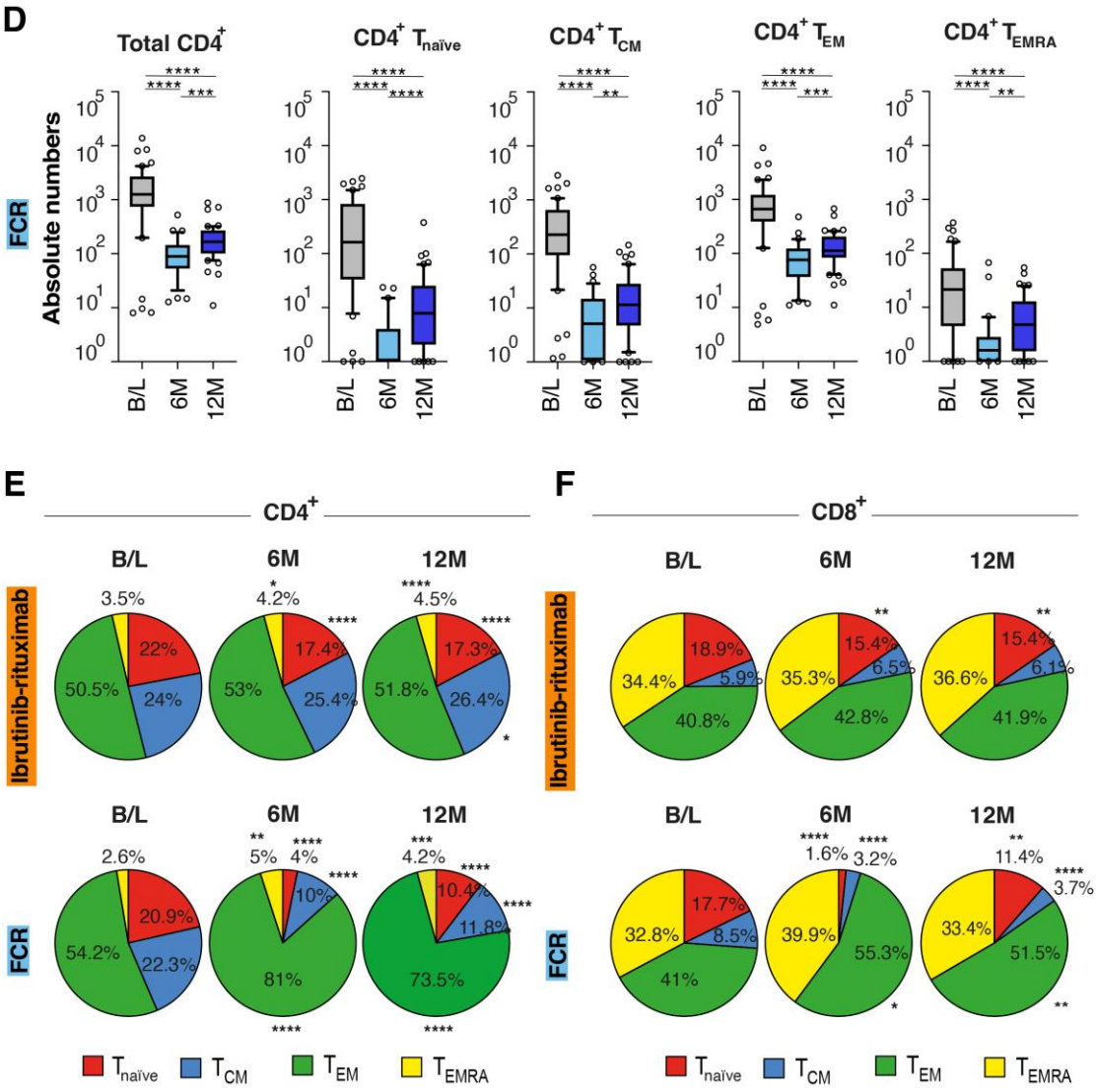

Supplemental Figure 2. Longitudinal impact of ibrutinib-rituximab and FCR therapy on CD8⁺ and CD4⁺ T cell subset numbers and frequency. Absolute numbers (number of cells / µl) of total, naïve ($CD45RA^+CCR7^+$), central memory (T_{CM}) ($CD45RA^-CCR7^+$) and terminally differentiated effector T_{EMRA} ($CD45RA^+$ $CCR7^-$) $CD8^+$ T cells in the (**A**) ibrutinib-rituximab (n=86) and (**B**) FCR (n=50) arm determined with flow cytometry. Data (log scale) are presented in Box and whiskers (10-90 percentile) plots. (**C**, **D**) Absolute numbers of $CD4^+$ T cell subsets determined with flow cytometry: naïve ($T_{naïve}$) ($CD45RA^+$ $CCR7^+$), central memory (T_{CM}) ($CD45RA^-$ $CCR7^+$), effector memory (T_{EM}) ($CD45RA^-$ $CCR7^-$) and terminally differentiated effector T_{EMRA} ($CD45RA^+$ $CCR7^-$) at the time-points indicated [(**C**) ibrutinib-rituximab (n=86) or (**D**) FCR (n=50)]. Results are the mean ± SEM from all CLL patient samples for each treatment arm. Differences between B/L

and on-treatment samples and between the 6- and 12- month time-points were assessed using the Wilcoxon signed-rank test. Frequencies of (**E**) $CD4^+$ and (**F**) $CD8^+$ T cell subsets of ibrutinib-rituximab and FCR treated samples calculated as the percentage (%) of CD4/8 subsets ($T_{naïve}$, T_{CM}, T_{EM}, T_{EMRA}) out of total CD4/8 T cells per sample. Pie charts present the average % of CD4/8 subsets calculated from all patients per treatment arm (IR n=86, FCR n=50). **P*<.05; ***P*<.01; ****P*<.001; *****P*<.0001; n/s, not significant.

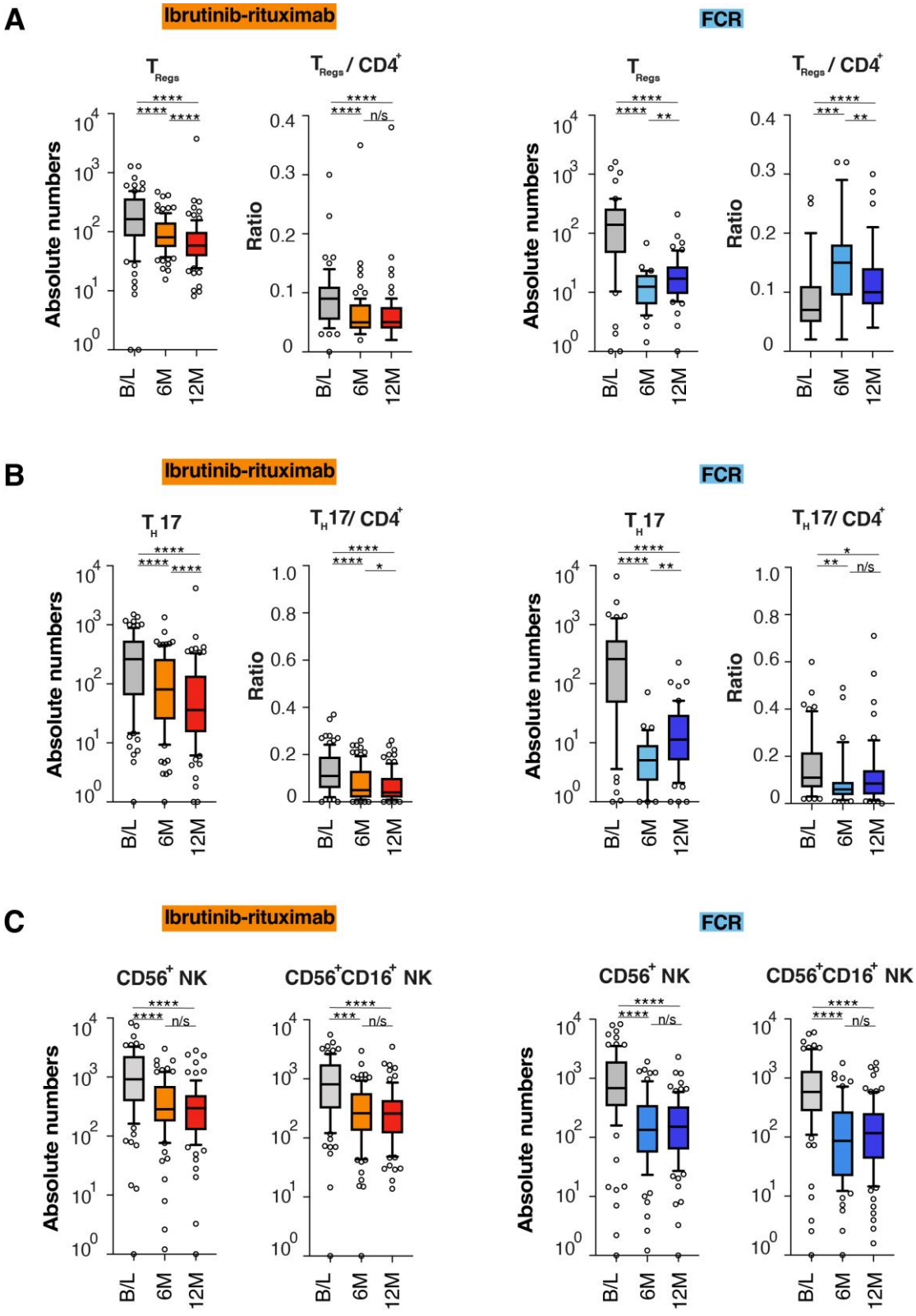

Supplemental Figure 3. Ibrutinib-rituximab and FCR therapy reduce absolute numbers of T_{Regs}, T_H17 and NK cells. Box and whiskers (10-90 percentile) plots of (A) absolute numbers (number of cells / µl) of T_{Regs} ($CD4^+CD127(dim)^+CD25^+$) and $T_{Regs}/CD4^+$ ratio, (B) absolute numbers

(number of cells / µl) of T_H17 ($CD4^+CXCR3^-CCR6^+$) and $T_H17/CD4^+$ ratio and (C) absolute numbers (number of cells / µl) of NK ($CD56^+CD3^-$) and $CD16^+$ NK cells in ibrutinib-rituximab (n=86) and FCR (n=50) treated samples. Results are the mean ± SEM from all CLL patient samples for each treatment arm. Differences were assessed by Wilcoxon signed-rank tests. *P<.05; **P<.01; ***P<.001; ****P<.0001; n/s, not significant.

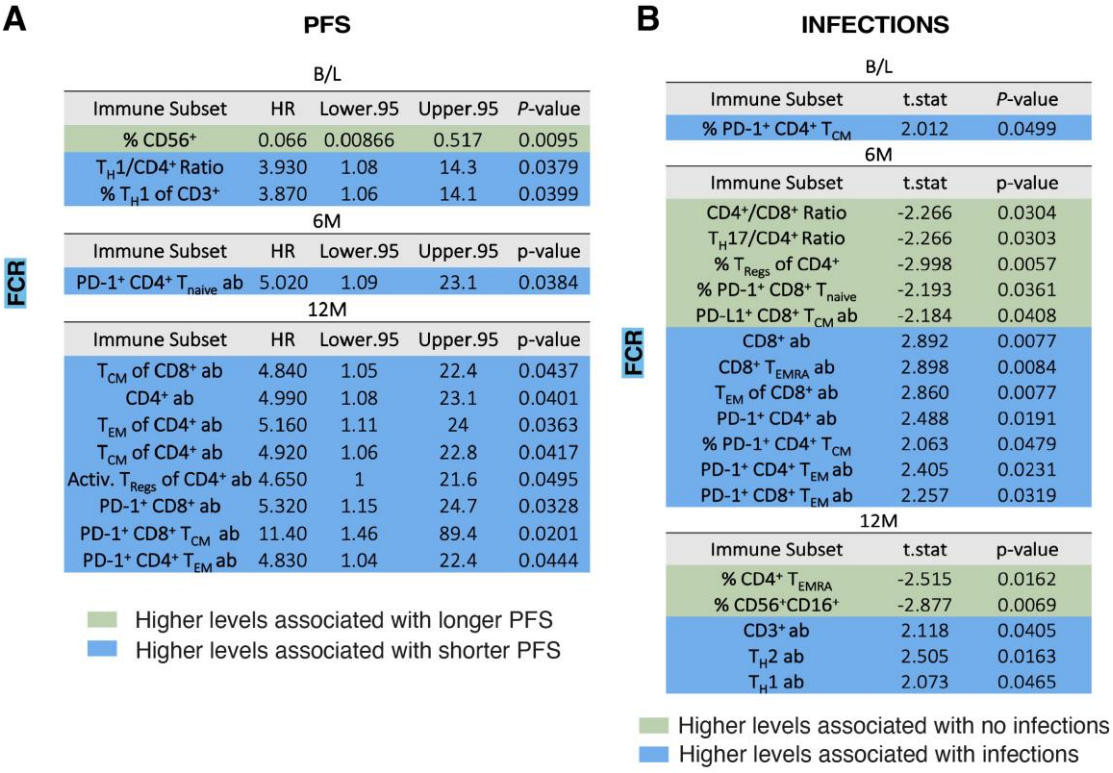

Supplemental Figure 4. Higher T cell subset levels associate with adverse PFS and infections in the FCR arm. (A) Table schematic summarizes the immune/T cell subsets that showed significant correlation (Cox model) between higher levels (flow cytometry analysis, median values used as cut-off point) and PFS during FCR (n=54 patients, with 13 experiencing disease progression). Green rows (correlations with Hazard Ratio (HR) values < 1) indicate higher immune subsets associated with good PFS, while higher immune subsets associating with adverse PFS (HR > 1) are highlighted in blue rows. Confidence intervals (95%) and P values

shown. (B) Schematic summarizing the significant correlations (Wilcoxon test) between immune subsets and infection (any infection) during FCR (n=54 patients). Negative t-statistics (t.stat) indicate higher immune subset levels in patients who did not develop infection (green rows). In contrast, correlations with a positive t.stat indicate higher immune subset levels in patients who developed infection (blue rows). Absolute number data is referred to as "ab". *P* values indicated.

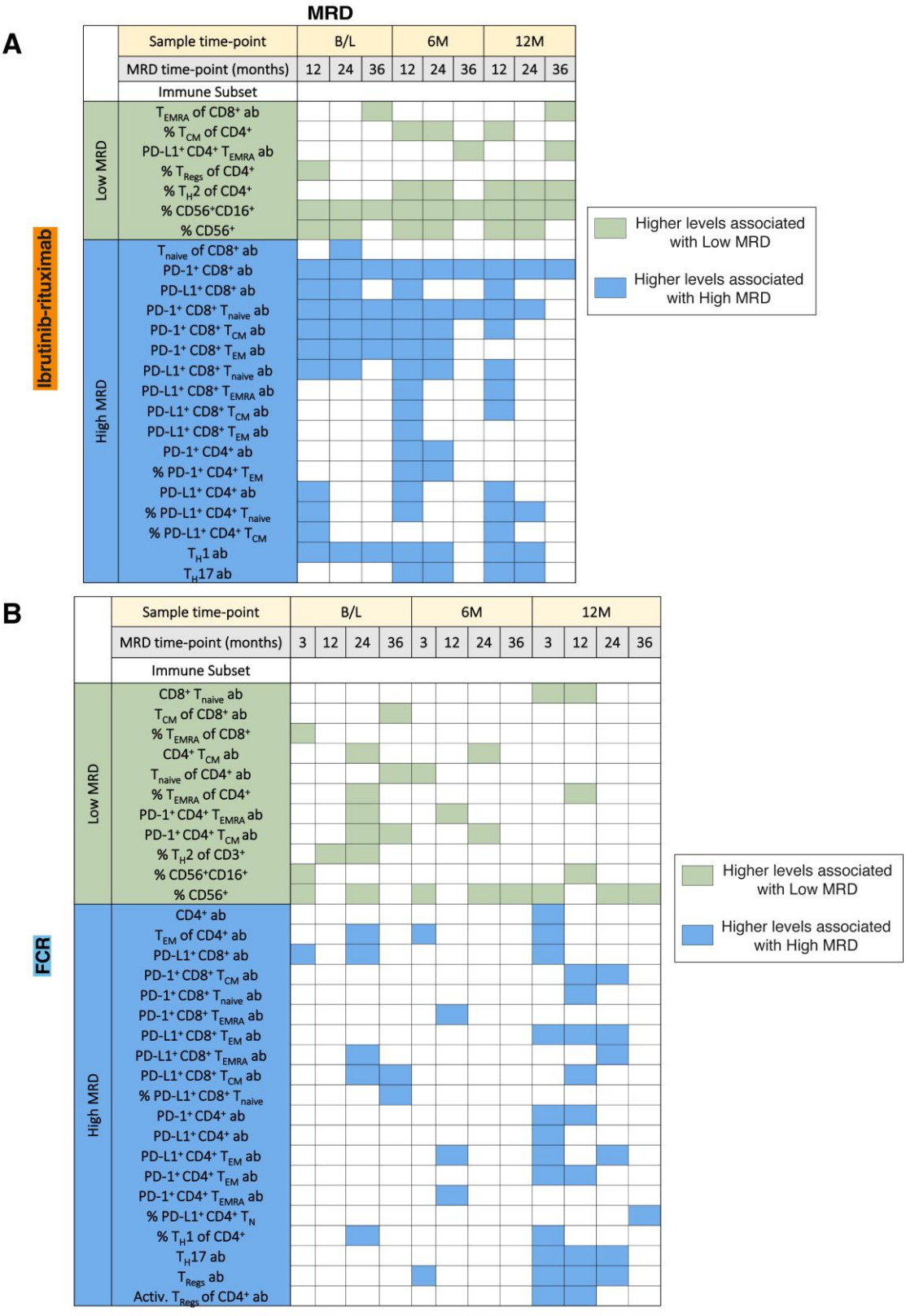

Supplemental Figure 5. Higher levels of T cell subsets and their immune checkpoint expression correlate with MRD levels during ibrutinib-rituximab, but less evident in the FCR arm. (A, B) Tables present the statistically significant Spearman correlations between higher immune/T

cell subset levels at B/L and 6M and 12M on-therapy (yellow row, sample time-points) and MRD levels measured at the indicated MRD measurement time-points (months) (grey rows) by flow cytometry for (**A**) Ibrutinib-rituximab n=88 patients; (**B**) FCR n=54 patients. Green rows/cells indicate higher immune subset levels in patients with low MRD levels (negative Spearman correlations). In contrast, blue rows/cells indicate higher immune subset levels in patients with higher MRD levels (positive Spearman correlations). *P*<.05. MRD, Minimal Residual Disease; ab, absolute number.

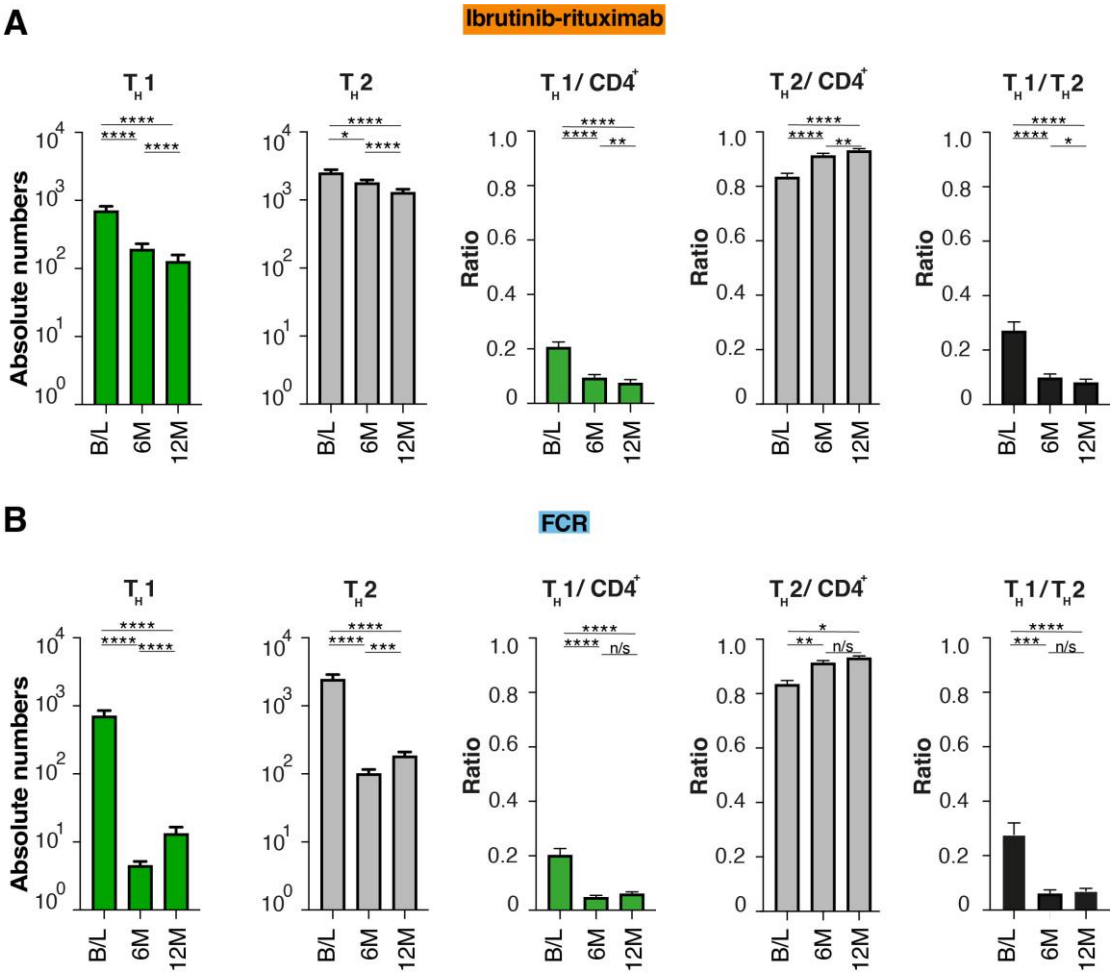

Supplemental Figure 6. Ibrutinib-rituximab and FCR therapy reduce the absolute numbers of T_H1 and T_H2 cell subsets. Absolute numbers (number of cells / µl) of T_H1 ($CD4^+CXCR3^+CCR6^-$) and T_H2 ($CD4^+CXCR3^-CCR6^-$) T cell subsets, $T_H1/CD4^+$, $T_H2/CD4^+$ and T_H1/T_H2 ratios of (**A**) ibrutinib-rituximab (n=86) or (**B**) FCR (n=50) treated samples determined by flow cytometry. Results are the mean ± SEM from all CLL patient samples for each treatment arm. Differences were assessed by Wilcoxon signed-rank tests. **P*<.05; ***P*<.01; ****P*<.001; *****P*<.0001; n/s, not significant.

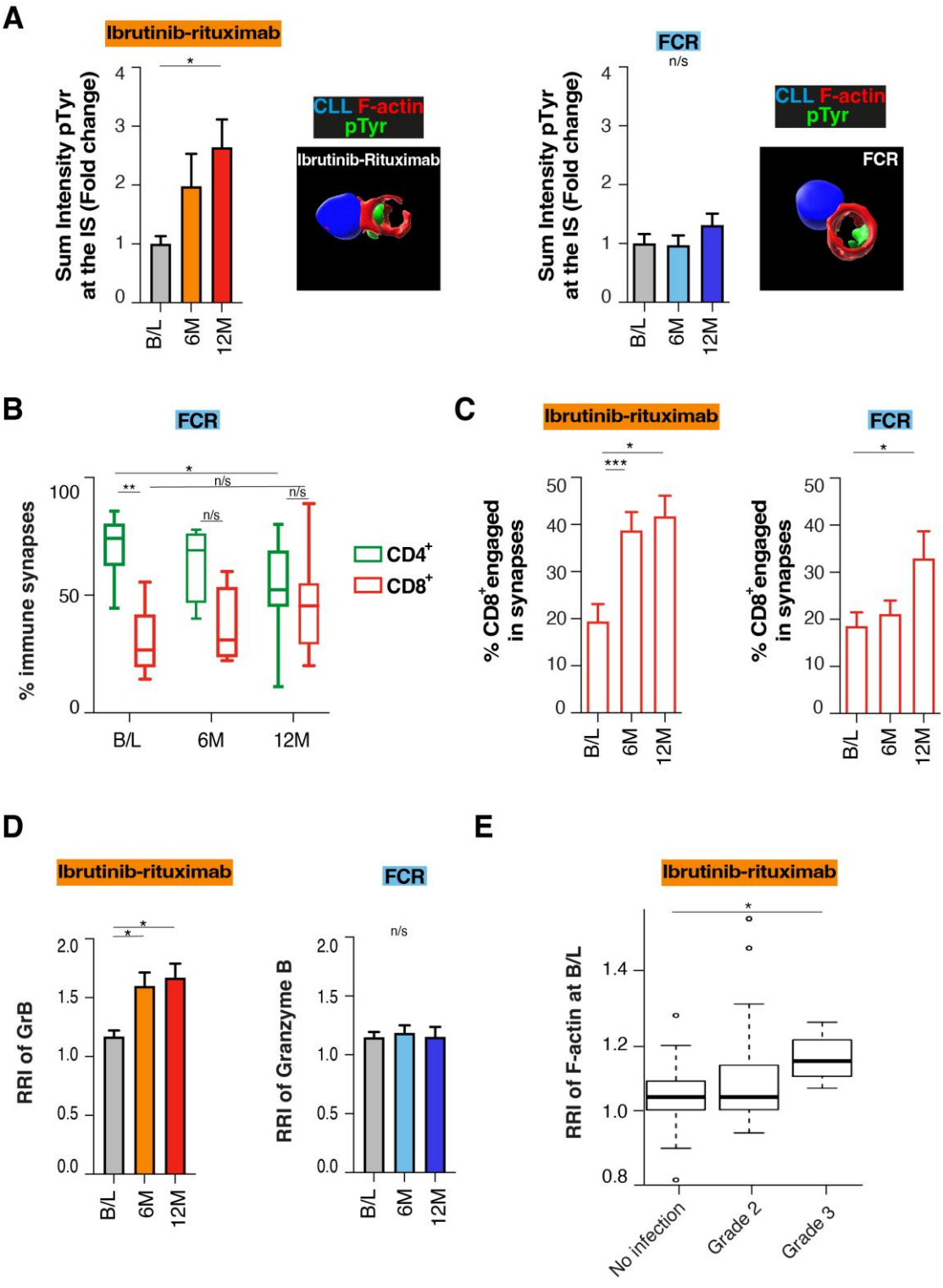

Supplemental Figure 7. Patient T cells show increased formation of granzyme B$^+$ CD8 T cell immune synapses during Ibrutinib-rituximab compared to clinically unfavourable CD4$^+$ T cell:CLL synapse interactions at baseline (prior to ibrutinib-rituximab) . (A) Quantification (mean ± SEM) of the polarized expression (Sum Intensity measurement) of TCR-mediated tyrosine-

phosphorylated proteins (pTyr, green fluorescent channel) at T cell:CLL contact sites/immune synapses during ibrutinib-rituximab and FCR therapy (longitudinal patient sample time-point analysis). PTyr data from the treatment time-points were normalized to the untreated B/L control levels (fold change) for each patient. (**B**) Box and violin plots (Min-Max) showing the percentage (%) of $CD4^+$ or $CD8^+$ T cell:CLL conjugates formed from the total/all T cell:CLL conjugates/immune synapses formed at B/L or at 6M and 12M following FCR therapy (n=11 patients). (**C**) % of $CD8^+$ T cells engaged in immune synapses with autologous B/L CLL cells at B/L or during ibrutinib-rituximab or FCR therapy (ibrutinib-rituximab: n=13, FCR: n=11). (**D**) Quantification of Granzyme B recruitment (RRI analysis) in $CD8^+$ T cell:CLL conjugates at B/L and during ibrutinib-rituximab and FCR time-points (n=10 patients per treatment arm). (**E**) The association between $CD4^+$ T cell F-actin polarization (RRI) immune synapse levels at baseline (B/L) and patients' infection status during ibrutinib-rituximab (no infection and grade 2 or 3 infections) (*, Wilcoxon test, P=.02). *P<.05; ***P<.001; n/s, not significant. Differences between B/L and 6- or 12-month time-points were assessed by Wilcoxon signed-rank test for all data sets (A, C, D) or multiple comparisons mixed effect ANOVA (B). Bar chart data presented as mean ± SEM.

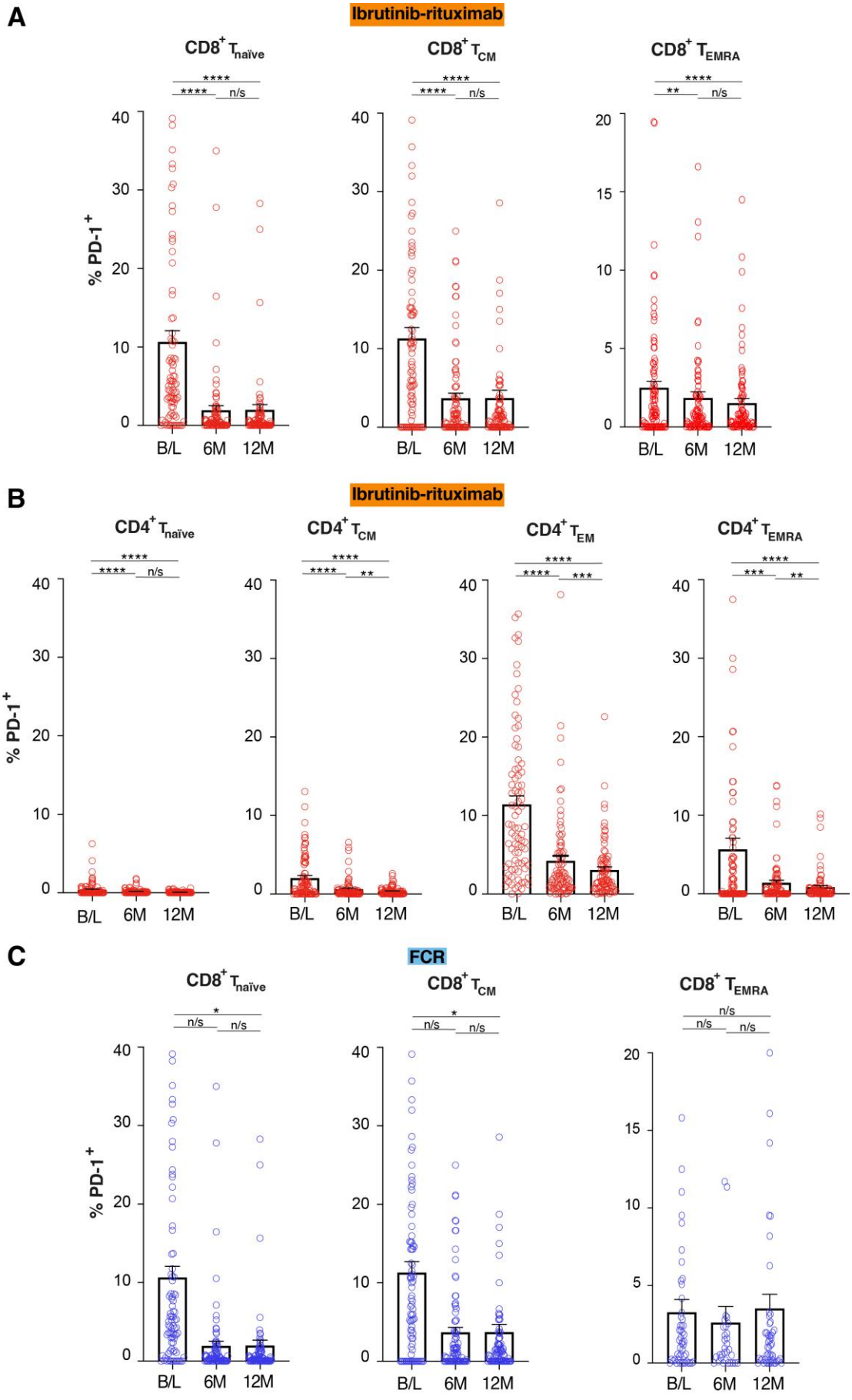
A
Ibrutinib-rituximab
CD8+ Tnaïve
CD8+ TCM
CD8+ TEMRA
% PD-1+
B/L
6M
12M
B
Ibrutinib-rituximab
CD4+ Tnaïve
CD4+ TCM
CD4+ TEM
CD4+ TEMRA
C
FCR
CD8+ Tnaïve
CD8+ TCM
CD8+ TEMRA

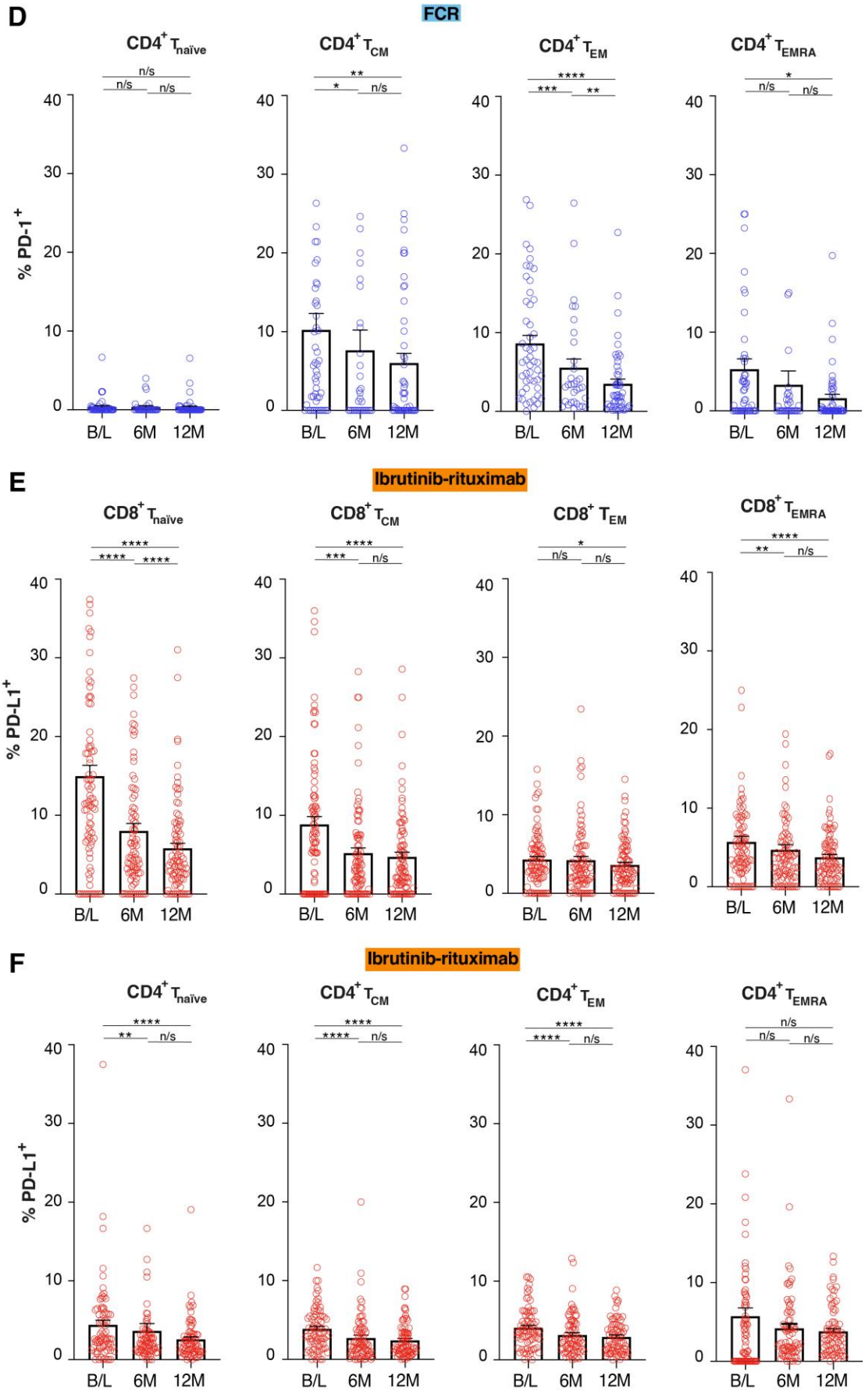
D
FCR
CD4+ Tnaïve
CD4+ TCM
CD4+ TEM
CD4+ TEMRA
% PD-1+
B/L
6M
12M
E
Ibrutinib-rituximab
CD8+ Tnaïve
CD8+ TCM
CD8+ TEM
CD8+ TEMRA
% PD-L1+
F
Ibrutinib-rituximab
CD4+ Tnaïve
CD4+ TCM
CD4+ TEM
CD4+ TEMRA
% PD-L1+

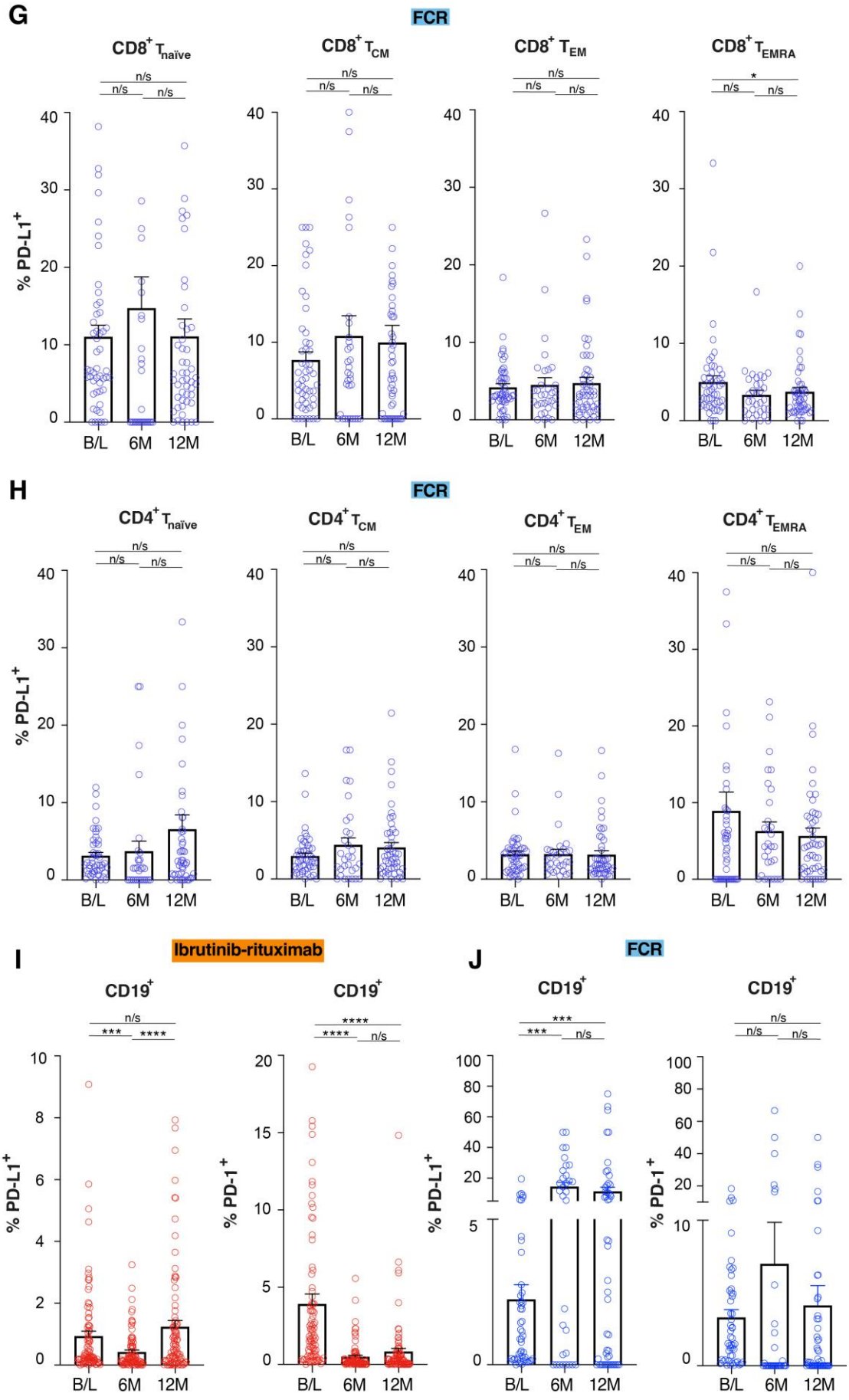
G
FCR
CD8+ TnaïveCD8+ TCMCD8+ TEMCD8+ TEMRA
% PD-L1+
n/s
*
B/L
6M
12M
H
FCR
CD4+ TnaïveCD4+ TCMCD4+ TEMCD4+ TEMRA
% PD-L1+
I
Ibrutinib-rituximab
CD19+
% PD-L1+
% PD-1+
***
****
J
FCR
CD19+
% PD-L1+
% PD-1+

Supplemental Figure 8. Ibrutinib-rituximab reduces the frequency of PD-1$^+$ and PD-L1$^+$ CD8$^+$ and CD4$^+$ T cell subsets, whereas FCR therapy maintains PD-1/PD-L1 expression levels on T cells. Percentage (%) of PD-1$^+$ (**A**-**D**) and PD-L1$^+$ cells (**E**-**H**) among the indicated CD8$^+$ T cell subsets (ibrutinib-rituximab: **A**, **E**; FCR: **C**, **G**) and CD4$^+$ T cell subsets (ibrutinib-rituximab: **B**, **F**; FCR: **D**, **H**) at baseline (B/L), 6M and 12M time-points on ibrutinib-rituximab (n=86) or FCR (n=50) therapy. (**I**-**J**) Percentage (%) of PD-1$^+$ and PD-L1$^+$ CD19$^+$ cells at baseline (B/L), 6M and 12M time-points on (**i**) ibrutinib-rituximab (n=86) or (**j**) FCR (n=50) therapy. Results are plotted using box and whiskers (10-90 percentile) plots showing the mean ± SEM from all CLL patient samples for each treatment arm. Differences were assessed using Wilcoxon signed-rank tests as indicated. *P<.05; **P<.01; ***P<.001; ****P<.0001; n/s, not significant.

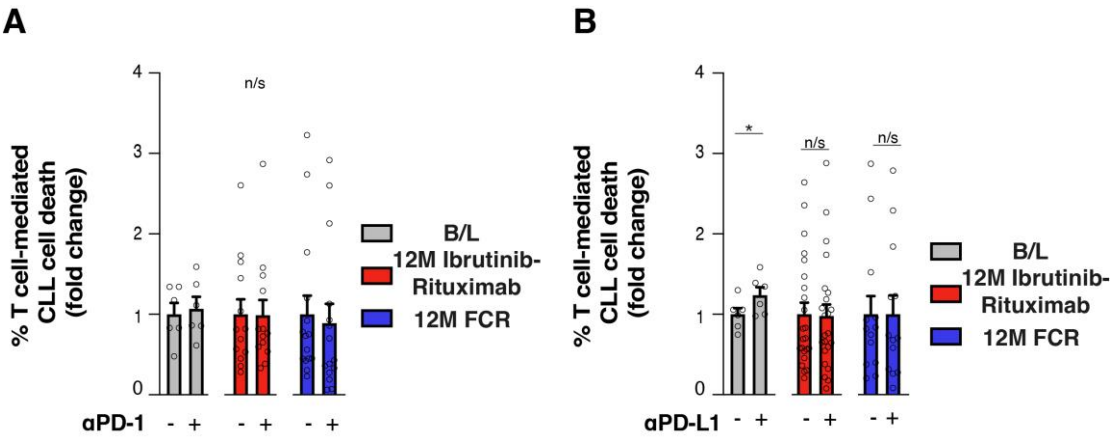

Supplemental Figure 9. *Ex vivo* treatment with anti-PD-1 or -PD-L1 immune checkpoint blocking antibodies does not improve anti-CLL T cell killing function using patient T cells from the 12-month treatment time-point following either ibrutinib-rituximab or FCR. T cell killing function against autologous CLL cells of T cells at baseline (B/L) or at the 12-month ibrutinib-rituximab (red) or FCR (blue) time-points following *ex vivo* treatment with (**A**) anti-PD-1 blocking antibody (αPD-1) or isotype control (indicated using "-") (B/L: n=6, ibrutinib-rituximab: n=13, FCR: n=15) or (**B**) anti-PD-L1 (αPD-L1) blocking antibody or isotype control (indicated using "-") (B/L: n=6,

ibrutinib-rituximab: n=23, FCR: n=13). Data were normalized to the isotype control treated samples (indicated as "-") and presented as fold change for each patient sample. Results are the mean ± SEM from all CLL patient samples for each arm. The addition of checkpoint treatment versus control was assessed using the Wilcoxon signed-rank test. *P<.05; n/s, not significant.